33rd Annual International Conference of the IEEE EMBS
Boston, Massachusetts USA, August 30 - September 3, 2011

Dynamic imaging of ictal rhythmic activity using dense-array EEG

Lin Yang, *Student Member IEEE*, Christopher Wilke, Benjamin Brinkmann, Gregory A. Worrell, Bin He, *Fellow IEEE*

***Abstract*— Electroencephalogram (EEG) is an important component of the pre-surgical evaluation in the treatment of medically intractable epilepsy. However, clinical EEG uses 19 to 32 electrodes that significantly limits its localization ability. Recent development of dense-array recording techniques has suggested that increased spatial sampling rate improves the accuracy of source localization. In the current study, we proposed a 76-channel EEG system for the long-term monitoring of epilepsy patients, and proposed a dynamic seizure imaging (DSI) technique to image the ictal rhythmic activity that may evolve through time, space and frequency. We tested the system in a cohort of 8 patients and our results show that the DSI estimated the seizure activity in good correlation with intracranial recordings, successful surgery outcomes and other clinical evidence. The proposed dense-array recording and DSI imaging approach enable a non-invasive but quantitative imaging of continuous seizure activity. The results suggest that DSI may potentially be useful to assist the pre-surgical evaluation in patients with intractable epilepsy.**

***Index Terms*— Dense-array EEG, Dynamic seizure imaging (DSI), Pre-surgical planning, Epilepsy.**

I. Introduction

Epilepsy is one of the most common neurological disorders that affects 1-2% of world population. In about 30% of patients suffering from epilepsy, seizures cannot be successfully controlled by medication alone. Surgery intervention removing or disconnecting the epileptogenic cortex becomes one of the last treatments for the cessation of or significant reduction of seizures.

EEG is an important component of the pre-surgical evaluation for the scalp mapping of seizure activity. The waveform of EEG is usually used to determine the lateralization or approximate localization of the seizure onset zone (SOZ). This procedure, however, suffers from low-spatial resolution due to the limited number of scalp electrodes (e.g., conventionally 19-32 electrodes in the clinical setting). To improve the spatial resolution, dense-array EEG techniques have been applied for the recording of inter-ictal events [1, 2] and most recently ictal events [3]. Studies demonstrated in inter-ictal spikes that increasing the number of scalp sensors would significantly increase the source localization accuracy [1, 4]. Development of source imaging techniques further improves the imaging capability of EEG by localizing the scalp events onto the underlying brain structures. While previous investigations have been successful, the dynamic imaging of seizure activity still remains a challenge in the field.

In this context, the present study aimed to develop a high-resolution seizure imaging approach for potential application in pre-surgical planning of the epilepsy treatment. We proposed a 76-electrode EEG monitoring system and a dynamic seizure imaging (DSI) technique. In a cohort of 8 patients, the dense-array EEG and DSI imaged seizure activity in good correlation with intracranial EEG (iEEG) and successful surgery outcomes. Such a seizure imaging tool characterizing high resolution in both time and space could significantly enhance pre-operative planning and have a major impact in the management of intractable epilepsy.

Manuscript received April 15, 2011. This work was supported by NIH RO1 EB007920, RO1 EB006433 and NSF CBET-0933067 (B.H.).

Yang L (yangx726@umn.edu), Wilke C, and He B (binhe@umn.edu) are with Department of Biomedical Engineering, University of Minnesota, Minneapolis, MN 55455 USA.

Brinkmann B, and Worrell G.A. are with Department of Neurology, Mayo Clinic, Rochester, MN USA

II. Materials and Methods

A. Subjects and Data Acquisition

We studied eight adult patients with medically intractable epilepsy. The procedure was approved by the Institutional Review Boards of the University of Minnesota (Minneapolis, MN) and Mayo Clinic (Rochester, MN). All the patients gave informed consent.

Each patient underwent a long-term video EEG monitoring using 76-channel system. Individual electrodes were glued over the scalp according to a 10-10 montage. The EEG recordings were referenced to CPz and sampled at 500 Hz. All

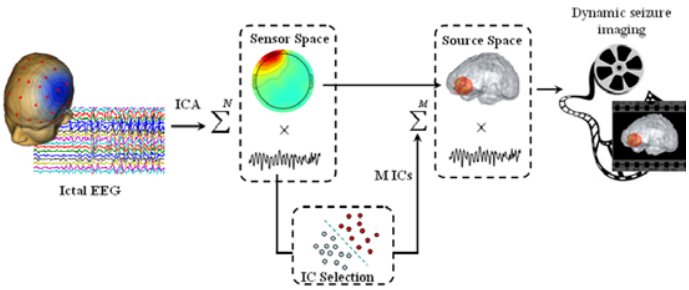

Fig. 1. Schematic diagram of the dynamic seizure imaging (DSI) approach.

the patients underwent a high-resolution 3.0T or 1.5T MRI anatomical scan. Three patients had iEEG recording. Seven patients underwent resective surgery and all became seizure free after one-year follow-up. They then had an additional MRI scan 3-4 months post-operatively. The other patient had iEEG and a single photon emission computerized tomography (SPECT) scan as part of the pre-surgical evaluation. Detailed patient information can be found in Table 1.

B. Dynamic seizure imaging

The relationship between multi-channel EEG signal Y and underlying brain activity S can be modeled by a linear system:

$$\mathbf{Y} = \mathbf{LS} + \mathbf{B} \quad (1)$$

where S is a source matrix, Y is a signal matrix and B is a noise matrix. L is a lead matrix, which can be calculated using the boundary element method (BEM) [5-7]. We used a BEM model consisting of three conductive layers: the brain, the skull and the skin with conductivity of 0.33 S/m, 0.0165 S/m and 0.33 S/m, respectively [8-10]. Around ten thousand equivalent current dipoles with unconstrained orientations were evenly distributed within the 3D brain volume to model the source space. Standard electrode positions were used for the calculation.

Seventeen seizures were identified by experienced clinical epileptologists and the seizure onset instants were determined. We segmented ictal EEG about 30-s before and following the seizure onset. Independent component analysis (ICA) was used to separate each ictal EEG into a series of temporally independent but spatially fixed components [11-13]:

$$\mathbf{Y} = \mathbf{QT} = \sum^{N} \mathbf{Q}_i \mathbf{T}_i \quad (2)$$

where $\mathbf{Q}_i$ is the spatial map of the *i*th IC, and $\mathbf{T}_i$ is the time course of the *i*th IC. N is the number of independent components (ICs). In ICA, the N we used equals to 80% of the number of electrodes.

The time-frequency change of ictal rhythmic activity is observable in raw EEG and also in the time course $\mathbf{T}_i$ of the independent components [11, 12]. Here, we used the correlation between the time-frequency patterns of EEG and ICs to select seizure components. For each seizure, the noise-deducted EEG was firstly constructed by removing artifatual components [14, 15]. The mean time-frequency representation (TFR) of EEG (EEG-TFR) and TFRs of each IC (IC-TFR) were calculated using sliding window short time Fourier transformation. Statistical significance of the correlation between EEG-TFR and each IC-TFR was quantified using a surrogate method [16, 17]. Statistically significant components were selected for further source analysis. Other component selection methods such as clustering techniques can be easily incorporated into the framework of DSI for various applications of different studies.

If M out of N ICs can be identified as seizure components, solving an EEG inverse problem from Y give the estimation of source activity, as:

TABLE I
PATIENT INFORMATION

Patient	Gender	Age	Surgery & Outcome
1	F	22	Surgery: L. FC Outcome: ILAE-1
2	M	32	Surgery: L. ATL Outcome: ILAE-1
3	M	58	Surgery: R. ATL Outcome: ILAE-1
4	F	28	Surgery: L. TL Outcome: ILAE-1
5	F	45	Surgery: R. TL Outcome: ILAE-2
6	M	49	Surgery: L. TL Outcome: ILAE-1
7	F	50	Surgery: R. TL Outcome: ILAE-1
8	M	36	N/A

Left (L.), right (R.), ILAE (International League against epilepsy), Anterior temporal lobectomy (ATL), Frontal cortectomy (FC), Temporal lobectomy (TL).

$$\hat{\mathbf{S}} = \mathbf{L}^{-1} \sum_{i=1}^{M} \mathbf{Q}_i \mathbf{T}_i = \sum_{i=1}^{M} (\mathbf{L}^{-1} \mathbf{Q}_i) \mathbf{T}_i = \sum_{i=1}^{M} \hat{\mathbf{S}}_i \mathbf{T}_i \quad (3)$$

where $\hat{\mathbf{S}}_i$ is the source of the ith IC, which can be estimated by solving inverse problems. Different source imaging algorithms such as Low Resolution Electromagnetic Tomography (LORETA) [18], minimum norm, weighted minimum norm, or fMRI-weighted minimum norm [19] can be easily incorporated by just change the inverse operator $\mathbf{L}^{-1}$. The spatiotemporal source estimation $\hat{\mathbf{S}}$ can be formulated as a linear combination of ICs in the source space, which can be seen as an inverse process of ICA. Since ICA separated signals according to maximal independence rather than absolute independence between signals, the step of re-combination could combine sources that are partially overlapped with each other.

The DSI approach provides a source estimation of $\hat{\mathbf{S}}$, which is a spatiotemporal signal with temporal resolution as high as EEG signal. Continuous change of seizure source distribution can be visualized as $\hat{\mathbf{S}}(\boldsymbol{r}, \boldsymbol{t} = \boldsymbol{t}')$, where t' refers to the time instant of interest. Similarly, source wave form at any brain voxel of interest r' can be extracted as $\hat{\mathbf{S}}(\boldsymbol{r} = \boldsymbol{r}', \boldsymbol{t})$.

III. RESULTS

Using ICA, multiple ICs can be identified from each seizure. Fig. 2(a) shows the biggest ICs identified from two seizures of a patient with frontal lobe seizure. The TFRs show increased rhythmic activity at seizure onset progressing to alpha band discharges, which is consistent with independent observation of experienced epileptologists. The spatial maps indicate activity in the left frontal electrodes. Fig. 2(b) shows two example ICs identified from two patients with temporal lobe seizure. Their TFRs show two different patterns, which are also observed in other patients with temporal lobe seizure. One pattern shows initial delta activity later progressing to theta band activity, and the other shows initial theta activity.

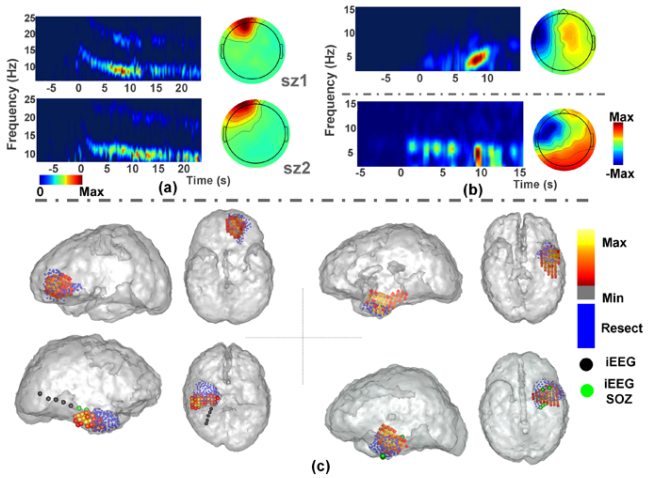

Fig. 2. (a) Time-frequency representations and scalp maps of two biggest ICs identified in two seizures in a patient with frontal lobe seizure. (b) Two example ICs from two patients with temporal lobe seizure. (c) Examples of DSI-estimated SOZs in 4 patients in comparison with surgically removed brain regions (blue) and SOZs delineated using iEEG (green electrodes). Black electrodes represent electrodes not involved in the seizure onset. Those electrodes were not plotted in the 4th one because the dense intracranial electrodes cover a big region of the brain surface.

The spatial maps indicate activity in the left temporal electrodes.

Given the estimated spatiotemporal source signal $\hat{\mathbf{S}}(\boldsymbol{r},\boldsymbol{t})$, the SOZ can be visualized as the source distribution at the seizure onset time determined by experienced epileptologists. Fig. 2(c) shows examples of the estimated SOZ (yellow-to-red color bar) in comparison with surgically resected regions (blue) and SOZs delineated by epileptologists using iEEG (green electrodes) in four patients. Upon visual inspection, the estimated SOZs are in good correlation with epileptogenic focus resected in the surgery and also with SOZs identified using iEEG, if available. One patient who did not have surgery underwent a SPECT scan and iEEG recording. The estimated SOZ is also in good agreement with the SPECT foci and iEEG foci. The peaks of the estimated SOZs of 14 seizures are localized within the surgically resected regions, whereas in the remaining 3 seizures the peaks are 0.99±0.16-cm away from the border of the resection. In most of the seizures, the estimated SOZs are concordant with the epileptogenic lobe, whereas small regions of false positive outside the epileptogenic lobe are observed in 2 seizures. In a group level, significant spatial overlapping between the estimated SOZs and the surgically resected regions is achieved in the seizures analyzed (Fig. 3b). The receiver operating characteristic (ROC) curve [20] and the area under the ROC curve (AUC) also show good consistency between the estimated SOZs and surgically resected regions (Fig. 3b). We applied source imaging on raw EEG data in a period of -50 ~ 50 ms of the seizure onset and selected the source distribution best correlated with the resected region for calculation of spatial overlapping and AUC index. The comparison shows that DSI achieved better performance than directly applying source imaging on raw EEG data (Fig. 3b).

Given the spatiotemporal signal $\hat{\mathbf{S}}(\boldsymbol{r},\boldsymbol{t})$, dynamic change of ictal rhythmic activity can be viewed as a movie over time. Fig. 3(a) shows an example of the time-varying source spectral power distribution of the ictal rhythm in 1-s time window of one patient with temporal lobe seizure. The source distribution over time suggests that the seizure activity starts from left temporal lobe and propagates to the parietal lobe and right temporal lobe later. Although a 1-s time window was used here for presentation, the time-varying source distribution can be visualized in a much finer time scale, because the estimation $\hat{\mathbf{S}}(\boldsymbol{r},\boldsymbol{t})$ has a temporal resolution as high as the original EEG signal.

IV. Conclusion and Discussion

In this study, we have proposed a new 76-channel EEG for long-term monitoring of epilepsy patients. The feasibility of the 76-channel long-term EEG monitoring has been demonstrated in a cohort of 8 patients. The EEG in this study was recorded over 5.5±3.2 days that successfully captured each clinic event, producing a yield rate of 100%. The mounting of the 76 electrodes only required 60 minutes preparation time by two experienced medical staff in contrast to 30 minutes for the preparation of a standard 32-channel clinical EEG. Previous studies have reported a dense-array but fast-capping EEG technique for which the preparation time can be as short as 15 minutes [3]. However this technique is limited by relatively shorter recording time (2-3 days) because the patients cannot comfortably wear the cap for long-term [3]. The 76-channel EEG, on the other hand, other than the additional electrodes, was identical with the conventional clinical EEG whose feasibility of long-term monitoring has been demonstrated over several decades' worth of clinical practice.

Another innovation of the present work is the proposed dynamic source imaging algorithm. In order to image the dynamic change of seizure activity, many efforts have been made, such as the application of dipole fitting techniques [21, 22] and the recent development of sub-space scanning techniques [23, 24]. Using distributed source model, a straightforward method is conducting source imaging instant by instant for each millisecond or for each short time window [3, 25], which can involve extensive computation. A previous study [26] improved the analysis of ictal EEG by decreasing the complexity of seizure data using the concept of "microstates". Here we proposed a novel dynamic source imaging technique which images the continuous change of ictal rhythmic activity with high spatiotemporal resolution. Using this decomposition-and-recombination process, regardless of the length of continuous ictal data, we can achieve a spatiotemporal imaging by solving a limited number (equal to the number of selected seizure components) of inverse problems, which decreases the complexity of computation. Also, the separation of seizure components from artifacts, noise and other background brain oscillations largely

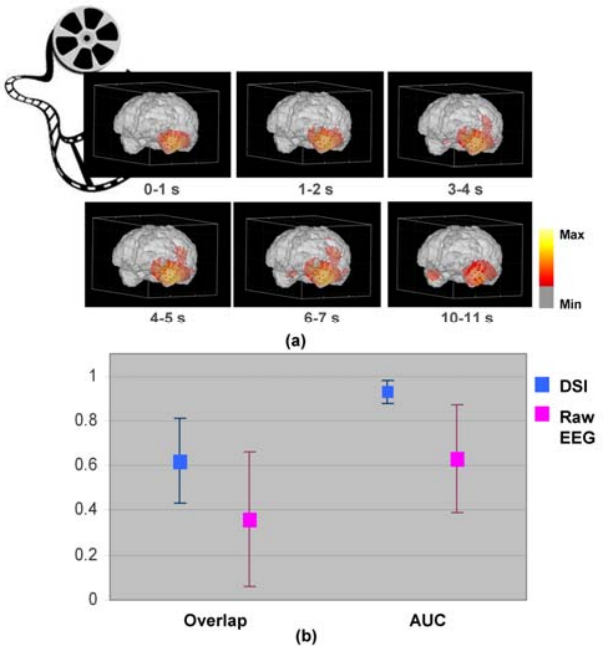

Fig. 3. (a) An example of the source distribution in 1-s time window after seizure onset in a patient. (b) In group level, the DSI-estimated SOZs showed better overlapping and consistency with surgically resected regions than directly applying source imaging on raw EEG data. The 'Overlap' is defined as the overlapped volume of the estimated SOZ with the resected region normalized by the size of the resected region.

enhances the source analysis and allows us to focus the analysis on dynamic change of ictal rhythms.

As imaging of seizure sources is the ultimate goal for surgical planning in epilepsy, the present study opens a new approach for epilepsy source localization. Compared with most other approaches where source localization is performed in interictal EEG or magnetoencephalogram (MEG), the present approach enables us to directly localize and image the dynamic seizure activity from seizure EEG. The high degree of concordance with successful surgical resection in the patient group indicates the promise and potential of this innovative methodology for surgical planning in epilepsy patients.

ACKNOWLEDGMENT

The authors would like to thank Cindy Nelson for technical assistance in data collection, and Dr. Gang Wang for assistance in data analysis.

REFERENCES

[1] G. Wang, G. Worrell, L. Yang, C. Wilke and B. He. (2010, Nov 30). Interictal spike analysis of high-density EEG in patients with partial epilepsy. Clin. Neurophysiol. .

[2] C. M. Michel, G. Lantz, L. Spinelli, R. G. de Peralta, T. Landis and M. Seeck, "128-channel EEG source imaging in epilepsy: clinical yield and localization precision," Journal of Clinical Neurophysiology, vol. 21, pp. 71-83, 2004.

[3] M. D. Holmes, D. M. Tucker, J. M. Quiring, S. Hakimian, J. W. Miller and J. G. Ojemann, "Comparing Noninvasive Dense Array and Intracranial Electroencephalography for Localization of Seizures," Neurosurgery, vol. 66, pp. 354-362, 2010.

[4] G. Lantz, R. Grave de Peralta, L. Spinelli, M. Seeck and C. Michel, "Epileptic source localization with high density EEG: how many electrodes are needed?" Clinical Neurophysiology, vol. 114, pp. 63-69, 2003.

[5] M. Hamalainen and J. Sarvas, "Realistic conductivity geometry model of the human head for interpretation of neuromagnetic data," IEEE Transactions on Biomedical Engineering, vol. 36, pp. 165-171, 1989.

[6] M. Fuchs, R. Drenckhahn, H. Wischmann and M. Wagner, "An improved boundary element method for realistic volume-conductor modeling," IEEE Transactions on Biomedical Engineering, vol. 45, pp. 980-997, 1998.

[7] B. He, T. Musha, Y. Okamoto, S. Homma, Y. Nakajima and T. Sato, "Electric dipole tracing in the brain by means of the boundary element method and its accuracy," IEEE Transactions on Biomedical Engineering, pp. 406-414, 1987.

[8] Y. Lai, W. Van Drongelen, L. Ding, K. Hecox, V. Towle, D. Frim and B. He, "Estimation of in vivo human brain-to-skull conductivity ratio from simultaneous extra-and intra-cranial electrical potential recordings," Clinical Neurophysiology, vol. 116, pp. 456-465, 2005.

[9] T. F. Oostendorp, J. Delbeke and D. F. Stegeman. "The conductivity of the human skull: Results of in vivo and in vitro measurements," Biomedical Engineering, IEEE Transactions on 47(11), pp. 1487-1492, 2000.

[10] Y. Zhang, W. van Drongelen and B. He, "Estimation of in vivo human brain-to-skull conductivity ratio with the aid of intracranial electrical simulation," Appl. Phys. Lett., vol. 89, 2006.

[11] H. Nam, T. G. Yim, S. K. Han, J. B. Oh and S. K. Lee, "Independent component analysis of ictal EEG in medial temporal lobe epilepsy," Epilepsia, vol. 43, pp. 160-164, 2002.

[12] A. Patel, F. Alotaibi, W. T. Blume and S. M. Mirsattari, "Independent component analysis of subdurally recorded occipital seizures," Clinical Neurophysiology, vol. 119, pp. 2437-2446, 2008.

[13] A. Delorme and S. Makeig, "EEGLAB: an open source toolbox for analysis of single-trial EEG dynamics including independent component analysis," J. Neurosci. Methods, vol. 134, pp. 9-21, 2004.

[14] T. P. Jung, S. Makeig, M. Westerfield, J. Townsend, E. Courchesne and T. J. Sejnowski, "Removal of eye activity artifacts from visual event-related potentials in normal and clinical subjects," Clinical Neurophysiology, vol. 111, pp. 1745-1758, 2000.

[15] E. Urrestarazu, J. Iriarte, M. Alegre, M. Valencia, C. Viteri and J. Artieda, "Independent component analysis removing artifacts in ictal recordings," Epilepsia, vol. 45, pp. 1071-1078, 2004.

[16] M. Palus and D. Hoyer, "Detecting nonlinearity and phase synchronization with surrogate data," IEEE Engineering in Medicine and Biology Magazine, vol. 17, pp. 40-45, 1998.

[17] J. Theiler, S. Eubank, A. Longtin, B. Galdrikian and J. Doyne Farmer, "Testing for nonlinearity in time series: the method of surrogate data," Physica D, vol. 58, pp. 77-94, 1992.

[18] R. Pascual-Marqui, C. Michel and D. Lehmann, "Low resolution electromagnetic tomography: a new method for localizing electrical activity in the brain," International Journal of Psychophysiology, vol. 18, pp. 49-65, 1994.

[19] L. Yang, Z. Liu and B. He, "EEG-fMRI reciprocal functional neuroimaging," Clinical Neurophysiology, 121(8), pp. 1240-1250, 2010.

[20] C. Grova, J. Daunizeau, J. M. Lina, C. Benar, H. Benali and J. Gotman, "Evaluation of EEG localization methods using realistic simulations of interictal spikes," Neuroimage, vol. 29, pp. 734-753, 2006.

[21] B. A. Assaf and J. S. Ebersole, "Continuous source imaging of scalp ictal rhythms in temporal lobe epilepsy," Epilepsia, vol. 38, pp. 1114-1123, 1997.

[22] B. A. Assaf, K. M. Karkar, K. D. Laxer, P. A. Garcia, E. J. Austin, N. M. Barbaro and M. J. Aminoff, "Ictal magnetoencephalography in temporal and extratemporal lobe epilepsy," Epilepsia, vol. 44, pp. 1320-1327, 2003.

[23] J. C. Mosher, P. S. Lewis and R. M. Leahy, "Multiple dipole modeling and localization from spatio-temporal MEG data," IEEE Transactions on Biomedical Engineering, 39(6), pp. 541-557, 1992.

[24] L. Ding, G. A. Worrell, T. D. Lagerlund and B. He, "Ictal source analysis: localization and imaging of causal interactions in humans," Neuroimage, vol. 34, pp. 575-586, 2007.

[25] G. A. Worrell, T. D. Lagerlund, F. W. Sharbrough, B. H. Brinkmann, N. E. Busacker, K. M. Cicora and T. J. O'Brien, "Localization of the epileptic focus by low-resolution electromagnetic tomography in patients with a lesion demonstrated by MRI," Brain Topogr., vol. 12, pp. 273-282, 2000.

[26] G. Lantz, C. Michel, M. Seeck, O. Blanke, L. Spinelli, G. Thut, T. Landis and I. Rosen, "Space-oriented segmentation and 3-dimensional source reconstruction of ictal EEG patterns," Clinical Neurophysiology 112(4), pp. 688-697, 2001.-